Whell Rotation Speed Control of Electric Car with Kalman Filter and PID Method

Fadjar Nur Falaah [1], Alfian Ma'arif [2,*]
[1,2] Department of Electrical Engineering, Universitas Ahmad Dahlan, Yogyakarta, Indonesia
Email: [1] Fadjar1800022067@webmail.uad.ac.id, [2] author@email
*Corresponding Author

Abstract*—Robotic development is becoming a major focus in modern technology with important applications in areas such as industry, defense, healthcare, and transportation. Accurately controlling the rotation speed of a DC motor wheel is a challenge, especially with changing operating conditions and external disturbances. This research aims to develop a control system using Kalman Filter and PID (Proportional-Integral-Derivative) methods to achieve fast and stable response while reducing steady-state error. The Kalman Filter improves the accuracy of speed estimation by minimizing the effect of noise, while the PID controller corrects the error between setpoint and actual values through three parameters: proportional (Kp), integral (Ki), and derivative (Kd). Preliminary findings show that large values of variation ratio in the Kalman Filter with the ratio of motor 1 (R = 10.0, Q = 0.0001), motor 2 (R = 8.0, Q = 0.0001) lead to slow motor response. Optimization of PID parameters for motor 1 (Kp = 1.1, Ki = 8.1, Kd = 0.00036) and motor 2 (Kp = 1.1, Ki = 8.1, Kd = 0.00036) resulted in better performance with a rise time of 0.13 seconds, overshoot of 8.69, and steady-state error of -1.19%. Further testing with a disturbance using a hall magnetic rotary encoder sensor revealed that motor M1 had a rise time of 0.27 seconds and motor M2 had a rise time of 0.16 seconds. Both motors showed good response to the disturbance, although the recovery time needs to be improved. This study concludes that the use of a combination of Kalman Filter and PID controller improves the motor control accuracy, although a faster recovery time is required to stabilize the motor response.

Keywords*—Robotic Development; DC Motor; Wheel Rotation Speed; Kalman Filter; PID Controller Control System

I. INTRODUCTION

The development of robotics has become a primary focus in modern technology, with broad applications across various fields such as industry, defense, healthcare, and transportation. A critical component of robotic systems is the drivetrain, which includes electric motors, transmissions, and wheels that enable the robot to move effectively and efficiently. DC motors are frequently utilized in robotic systems due to their ability to provide high torque, ease of control, and relatively low cost. However, accurately controlling the rotational speed of the wheels poses a significant challenge, particularly when dealing with changes in operating conditions and external disturbances. Ineffective control systems can lead to inefficiency, instability, and accelerated wear and tear of components.

To address these challenges, a control system is required that can deliver rapid and stable responses, minimize steady-state errors, and effectively manage external disturbances and operational variability. Two techniques that have proven to be highly effective for this purpose are the Kalman Filter and the PID (Proportional-Integral-Derivative) controller.

The Kalman Filter is an algorithm designed to estimate the state of a system by reducing the impact of noise and disturbances on sensor data. In the context of wheel speed control, the Kalman Filter enhances the accuracy of DC motor speed estimation by leveraging measured data from sensors. This improved estimation can then be utilized by the PID controller to regulate motor speed more effectively. The PID controller, a well-established control method in various industrial and robotic applications, operates by correcting the error between the setpoint and the actual value through three parameters: proportional (Kp), integral (Ki), and derivative (Kd). When properly tuned, a PID controller can provide a rapid and stable response to changes in wheel speed.

The integration of the Kalman Filter with the PID controller in a robotic wheel speed control system is expected to offer several benefits, including enhanced control accuracy, reduced sensor noise effects, and improved overall system stability. This research aims to evaluate the performance of the combined Kalman Filter and PID controller in controlling the rotational speed of DC motor wheels in a robot, and to identify potential improvements in designing a more efficient and responsive drivetrain.

Through this study, it is anticipated that deeper insights will be gained into the application of advanced control methods in robotic drivetrain systems, ultimately contributing to the development of more efficient, reliable, and high-performing robots.

II. METHOD

A. Software designing

Software design in the study includes a flowchart of how the tool system works with kalman filter and PID methods, programming. Programming in this research uses a programming application in the form of ArduinoIDE software.

Flowchart diagram of kalman filter and PID, pushbutton, rotary encoder sensor (SRE), value (SP, Kp, Ki, Kd). When the potentio is given a PWM value of 0>50, the two DC motors will rotate according to the PWM value entered, and the sensor reads the motor speed angle which will enter the kalman filter calculation. Continued to the PID calculation which will produce an output value in the form of a PWM value of 0>50, then from these results will compare with the PWM value found on the potentiometer.

Then when the Y = 0˚ <> -45˚ steering wheel which has a hall incremental magnetic rotary encoder sensor will control

and provide interference to the two right and left motors along with the PWM value of the PID calculation, when the incremental photoelectric rotary encoder sensor is given the action of being deflected to the left or right will reduce the speed of the left and right DC motors, the system will loop according to how the system works.

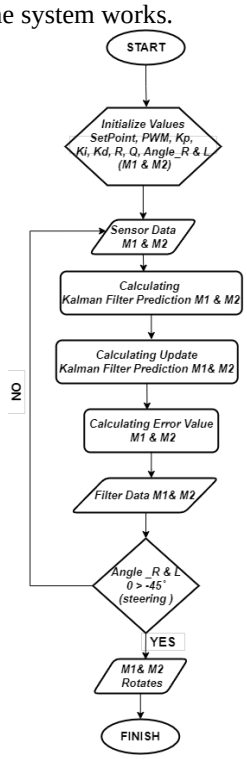

Fig. 1. Flowchart diagram system, Kalman Filter and PID method.

B. *Hardware designing*

Hardware design includes a system block diagram to provide an overview of the main system components used. The system block diagram in the design of electric car wheel speed control with kalman filter and PID methods is used as an initial design such as input, system output and system work processes in a row. This system block diagram uses the Arduino Mega 2560 microcontroller as an input and output processing tool for the entire system, and the voltage source used in this system comes from a 5V-12V 10 A power supply.

This is a system block diagram for reference to system design in order to facilitate research in carrying out the stages in a coherent manner.

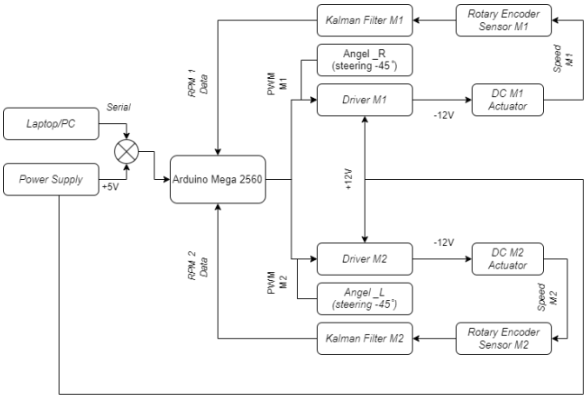

Fig. 2. Block Diagram System

Kalman filter and PID system control block diagrams are used for input and output system functions that can be described, such as reference values (setpoints) and speed sensors used as feedback. The speed angle of the DC motor will be detected by the speed sensor and compare the SP (setpoint) value with PV (present value) to obtain an error value that will be included in the PID control equation, from the calculation it produces an error value in the form of a PWM (Pulse Width Modulation) value and is forwarded to the BTS7960 driver, the motor driver will convert the PWM signal into an analog signal. The analog signal will drive the rotation of the DC motor and the rotation speed will be read by the speed sensor.

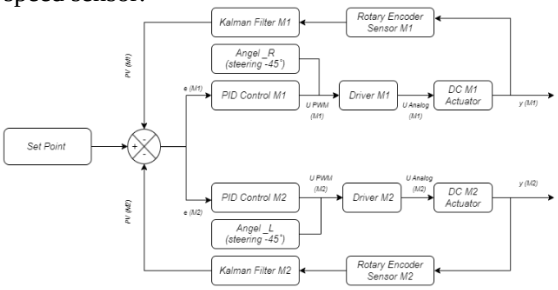

Fig. 3. Block Diagram Kalman Filter & PID

C. *Wiring Diagram*

The wiring diagram includes several input and output components connected to the Arduino MEGA2560 microcontroller such as hall incremental magnetic rotary encoder sensors, speed sensors, push buttons, potentiometers and outputs in the form of L298N drivers, 2x16 I2C LCDs, DC motors. The wiring diagram can be used for PCB (printed circuit board) making reference using Eagle software.

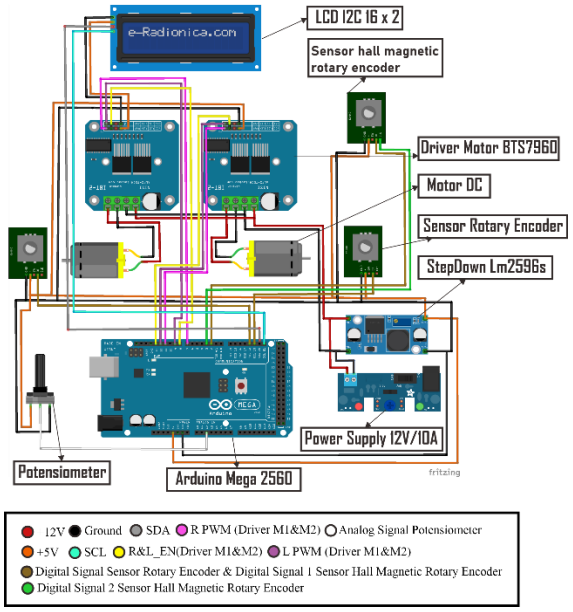

Fig. 4. Wiring Diagram

III. Result And Discussion

Research is carried out based on testing to get system data so that it can be known the workability of the system that has been designed, with reference to input voltage testing, RPM with Rotary Encoder Sensor (KY-040), PID Control Parameter Testing, PID Control Response Testing.

A. Output Voltage Testing Data

Output voltage testing on the BTS7960 motor driver (M1 & M2) is done by entering PWM variations 50> 250 with an arduino output voltage of 5V and a driver input voltage of 12.3 V. aims to determine the output voltage of the motor driver after being given a PWM variation using a digital multimeter measuring instrument. After the measurements are taken, the results of the motor driver output voltage.

The variation of the PWM value given affects the output voltage pin of the motor driver connected to the DC motor, there is an increase in voltage along with the variation of the PWM value given starting from 50, 75, 100, 125, 150, 175, 200, 225, 250. The difference in output voltage between M1 and M2 is seen at PWM 50 which can occur due to the program execution on the Arduino.

TABLE I. Output Voltage Testing Data

Output Voltage Testing Data			
No	PWM Value	Output Voltage(V)	
		M1	M2
1	50	2.4	2.5
2	75	3.6	3.6
3	100	4.8	4.8
4	125	6	6
5	150	7.2	7.2
6	175	8.4	8.4
7	200	9.6	9.6
8	225	10.8	10.8
9	250	11.9	11.9

B. RPM Testing Data with Rotary Encoder Sensor (KY-040)

In testing the rotary encoder sensor, calibration of the rotational speed of the DC motor is carried out using a digital tachometer with an interval specification of 0.8 milli / second. Testing of rotary encoder sensors is done by trial and error method, namely by providing input variations in PWM values of 50, 75, 100, 125, 150, 175, 200, 225, 250. In the Arduino program, a multiplier factor of 20.0 is used in the countPulseM1 variable of DC motor M1 and 40.9 in the countPulseM2 variable of DC motor M2, there is a difference in the multiplier factor due to the difference in pulse readings in one full rotation. Rotary encoder sensor testing data and the resulting calibration data can be seen in the table 2 below.

TABLE II. RPM testing against Tachometer

RPM testing against Tacometer							
No.	PWM	System		Tachometer		Error/Difference	
		M1	M2	M1	M2	M1	M2
1	50	118	164	120,8	131,6	2,8	32,4
2	75	183	209	183,8	200,5	0,8	8,5
3	100	232	270	239,0	273,0	7,0	3,0
4	125	289	349	310,5	344,7	21,5	4,3
5	150	322	416	369,4	412,8	47,4	3,2
6	175	409	452	433,4	478,0	24,4	26
7	200	435	486	491,8	553,5	56,8	67,5
8	225	542	553	550,7	621,7	8,7	68,7
9	250	629	695	632,4	725,2	3,4	30,2

In the table is the data from the tachometer reading and the rotary encoder sensor reading, where there is a very significant error value or difference due to the kalman filter response which is too slow, the response improvement is carried out using the PID method, it can be seen in the figure 6.

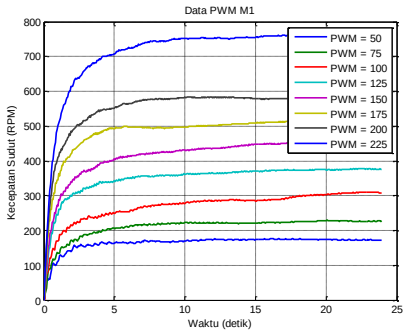

Fig. 5. Graph of RPM of motor M1 against PWM

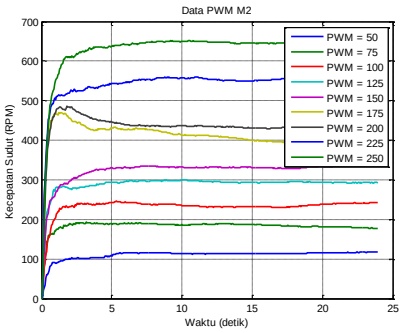

Fig. 6. Graph of RPM of motor M2 against PWM

C. *Kalman Filter Testing Data on PWM 50*

In testing the kalman filter method, variations in the value of parameters R and Q are tested. to get a minimal value with nois and produce a stable graph with a PWM range of 50 with the ratio of R and Q as found in the Table 3.

TABLE III. KALMAN FILTER M1& M2 RPM CALIBRATION

Kalman Filter M1 Rpm Calibration		
No.	R	Q
1	8	0.01
2	9.5	0.001
3	10	0.0001
Kalman Filter M2 Rpm Calibration		
No.	R	Q
1	7	0.01
2	7.5	0.001
3	8	0.0001

And the results of the R and Q M1 tests in the graph can be seen in the image :

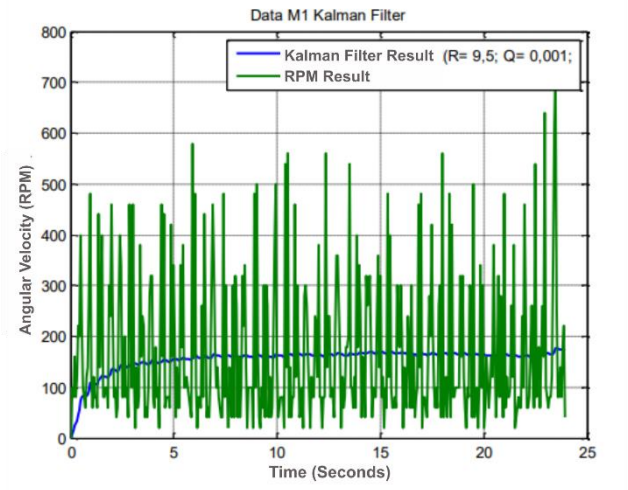

Fig. 7. M1 R =8, Q=0.01

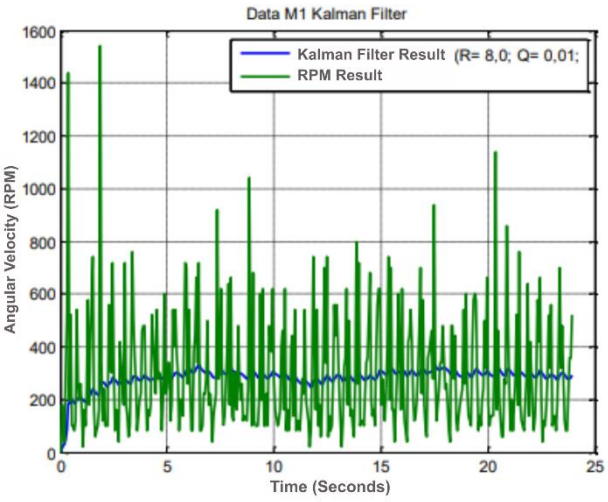

Fig. 8. M1 R=9.5, Q= 0.001

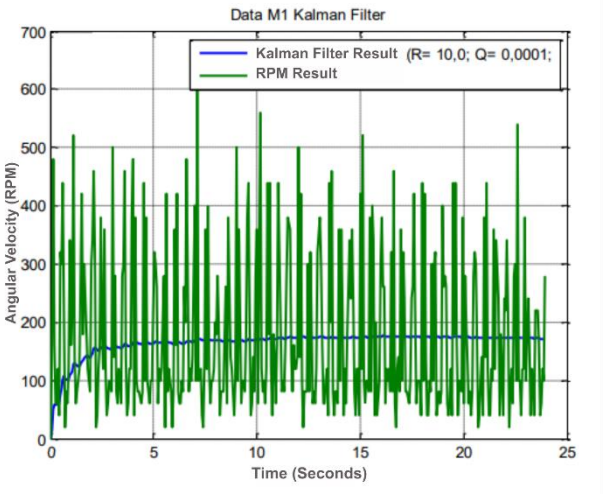

Fig. 9. M1 R=10, Q= 0.0001

Then the results of the R and Q M1 tests in the graph can be seen in the image:

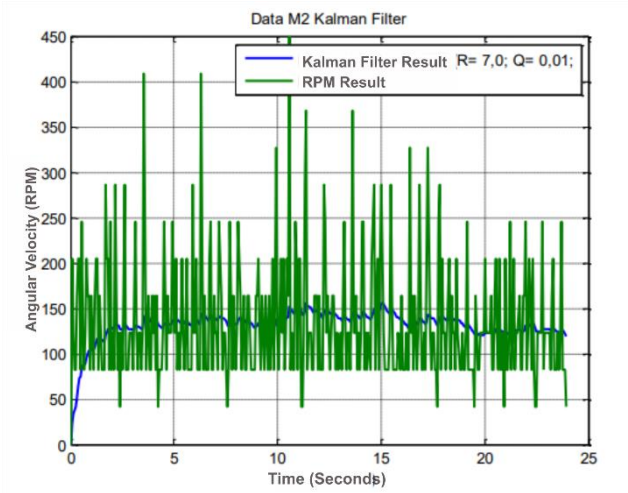

Fig. 10. M2 R =7, Q=0.01

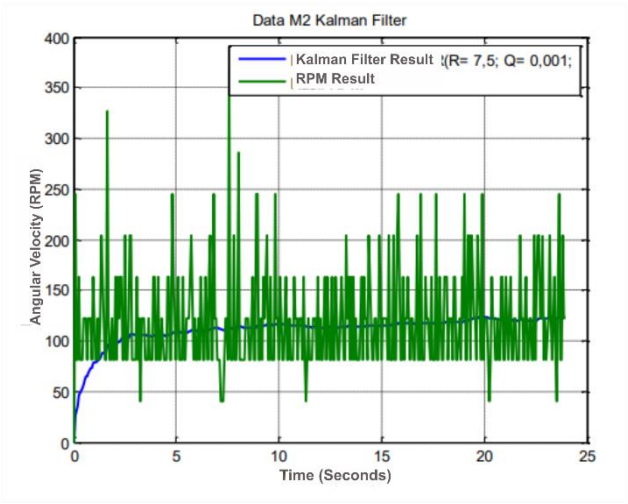

Fig. 11. M2 R =7.5, Q=0.001

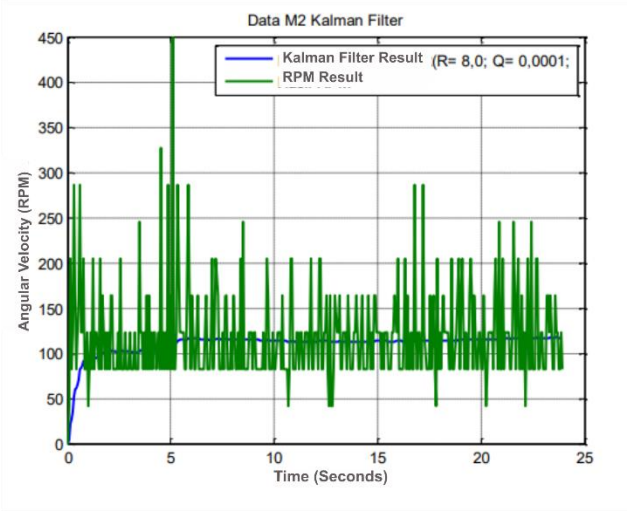

Fig. 12. M2 R =8, Q=0.0001

In the third test using the ratio R = 10; Q = 0.0001 on M1 reaches a stable time of 10/second and the ratio R = 8.0; Q = 0.0001 on M2 reaches a stable time of 5/second is the best ratio value that can reduce noise that is too high but the response is quite slow. Compared to the first and second tests with ratios R = 8.0; Q = 0.01 and R = 9.5; Q = 0.001 on M1 and ratios for M2 R = 7.0; Q = 0.01 and R = 7.5; Q = 0.001.

D. PID Controller Testing

Testing is done to improve the DC motor response after noise repair with the kalman filter method with the aim that the resulting response will be faster than without the PID method, there are several parameters used, namely Kp, Ki, Kd with sampling try and error as many as 5 times on each parameter.

1. KP Parameter Testing of Motor 1 and Motor 2

Kp parameter testing aims to determine the optimal value that produces fast and stable system response, reduces steady-state error, improves transient response, avoids overshoot and oscillation, ensures stability, and adapts to the specific characteristics of the system with several variations in Kp parameter values.

TABLE IV. PROPOTIONAL CONTROL TESTING ON M1

Propotional (P) control testing M1								
No .	Kp	Ki	Kd	Rise Time (Tr)	Overshoot (Mp)	Peak Time (Ts)	Settling Time (Ts)	Steady State error
1	0.7	0	0	NaN	0	NaN	NaN	28.94
2	0.8	0	0	NaN	0	NaN	NaN	22.96
3	0.9	0	0	NaN	0	NaN	NaN	19.04
4	1	0	0	0.98	0	103.58	NaN	15.78
5	1.1	0	0	0.2	0	99.14	NaN	19.22

In the Table 4 it can be seen that there are 5 sampling parameters Kp values 0,7; 0,8; 0,9; 1,0; 1,1. Produces a poor value which cannot reach the desired setpoint at a speed of 130 RPM, indicating that the steady state error value is still too large which is generated by the graph not reaching a steady state, plus the settling time value is not measurable because it does not reach the setpoint area. And can be seen the response of motor 1 in the form of a graph in Figure 14.

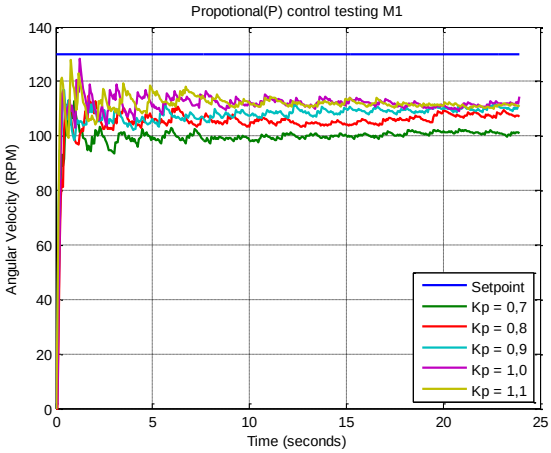

Fig. 13. Motor M1 Response Kp Graph

TABLE V. TESTING PROPOTIONAL CONTROL ON M2

Propotional (P) control testing M2								
No .	Kp	Ki	Kd	Rise Time (Tr)	Overshoot (Mp)	Peak Time (Ts)	Settling Time (Ts)	Steady State error
1	0.6	0	0	NaN	0	2.1	NaN	47.64
2	0.7	0	0	NaN	0	1.02	NaN	42.53
3	0.8	0	0	NaN	0	0.6	NaN	42.44
4	0.9	0	0	NaN	0	0.36	NaN	37.51
5	1	0	0	NaN	0	0.54	NaN	33.11

The Table 5 shows the variation of Kp testing parameters for motor 2 which is not much different from the results of motor 1 parameters, still too far from the desired setpoint value resulting in a settling time value and a relatively high steady state error value. And can be seen the response of motor 2 in the form of a graph in Figure 15.

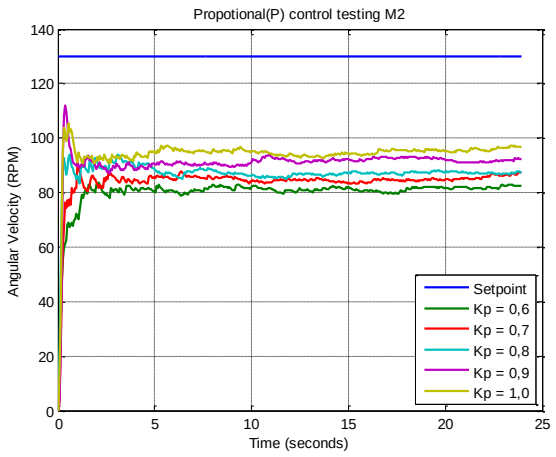

Fig. 14. Motor M2 Response Kp Graph

2. *KPI parameter testing on motor 1 and motor 2*

Kpi parameter testing aims to determine the optimal value that provides fast and stable system response, reduces steady-state error through error integration, improves transient response, avoids overshoot and oscillation, ensures stability, and adapts to the specific characteristics of the controlled system by varying the Kpi parameter value on motor 1 and motor 2. The variation of Kpi parameter value of motor 1 can be seen in Table 6 and motor 2 can be seen in Table 7.

TABLE VI. TESTING PROPOTIONAL INTEGRAL CONTROL ON M1

Propotiona Integral (PI) control testing M1								
No .	Kp	Ki	Kd	Rise Time (Tr)	Overshoot (Mp)	Peak Time (Ts)	Settling Time (Ts)	Steady State error
1	0.7	7.7	0	0.37	21.17	145.08	122.55	0.24
2	0.8	7.8	0	0.33	23.28	142.47	115.84	-1.47
3	0.9	7.9	0	0.41	19.75	145.2	121.79	-0.27
4	1	8	0	0.3	NaN	143.92	118.94	3.02
5	1.1	8.1	0	0.15	11.58	144.27	117.38	1.72

It can be seen from Table 6 that the response of motor 1 has reached the desired setpoint and the steady state error value is small but there is a high overshoot value for each parameter because it exceeds the 10% overshoot limit, so from such a high overshoot it is necessary to add the Kd parameter to stabilize the response of motor 1 and can be seen the response of motor 1 in Figure 16.

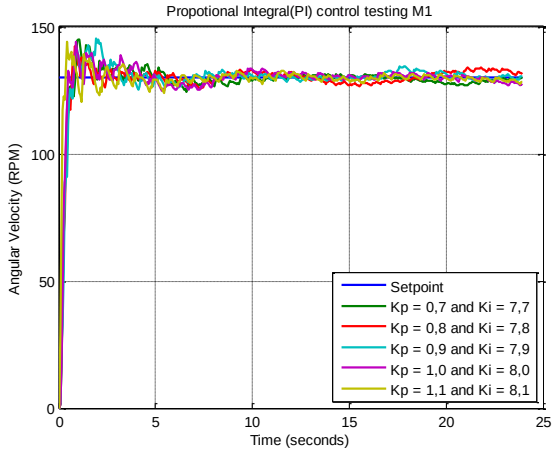

Fig. 15. Motor M1 Response Ki Graph

TABLE VII. TESTING PROPOTIONAL INTEGRAL CONTROL ON M2

Propotiona Integral (PI) control testing M2								
No .	Kp	Ki	Kd	Rise Time (Tr)	Overshoot (Mp)	Peak Time (Ts)	Settling Time (Ts)	Steady State error
1	0.6	9.1	0	0.1	68.61	0.3	17.52	-1.41
2	0.7	9.2	0	0.13	37.13	0.3	16.75	-0.3
3	0.8	9.3	0	0.07	103.36	0.24	11.2	1
4	0.9	9.4	0	0.08	96.1	0.24	15.18	0.87
5	1	9.5	0	0.06	219.23	0.24	9.86	2.85

It can be seen in Table 7 for the response of motor 2 the steady state error value drops but there is an overshoot value at each parameter variation given which exceeds the 10% limit, just like in the response of motor 1 it is necessary to add the Kd parameter. And the response of motor 2 can be seen in the form of a graph which can be seen in Figure 17.

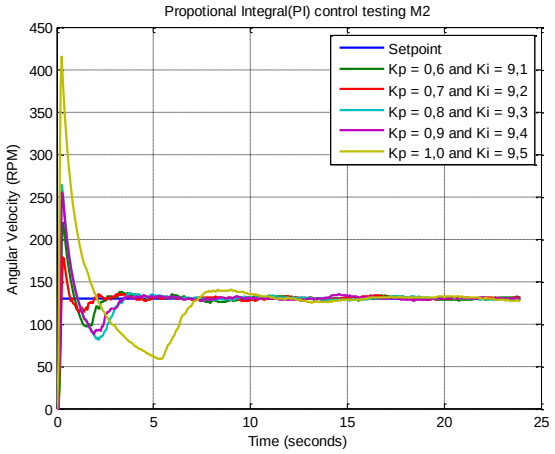

Fig. 16. Motor M2 Response Ki Graph

3. *KPID parameter testing*

After several tests of Kp and Kpi on the response of the two motors there is still a steady state error value, the overshoot is not good, so in this case it is necessary to add parameters to stabilize the response of the two motors to the desired setpoint. The following is a table of variant values of the first KPID value test can be seen in Table 8 for motor response 1.

TABLE VIII. TESTING PROPOTIONAL INTEGRAL DERIVATIVE (PID) CONTROL M1

Propotiona Integral Derivative (PID) control testing M1								
No .	Kp	Ki	Kd	Rise Time (Tr)	Overshoot (Mp)	Peak Time (Ts)	Settling Time (Ts)	Steady State error
1	0.6	9.1	0.00006	0.56	12.33	2.1	7.36	-0.88
2	0.7	9.2	0.00007	0.49	11.16	1.38	7.54	1.85
3	0.8	9.3	0.00008	0.34	15.41	0.54	20.22	-0.03
4	0.9	9.4	0.00009	0.38	5.5	2.88	13.24	-0.16
5	1	9.5	0.0001	0.25	7.67	0.6	21.72	0.73

Judging from Table 8 for motor response 1, the parameter values Kp = 1.1; Ki = 8.1; Kd = 0.00036 with a rise time of 0.13/second, overshoot 8.69; peak time 141.62; 11.4%, and steady state error -1.19. The time to stabilize is faster than the other parameters. And can be seen in graphical form in Figure 18.

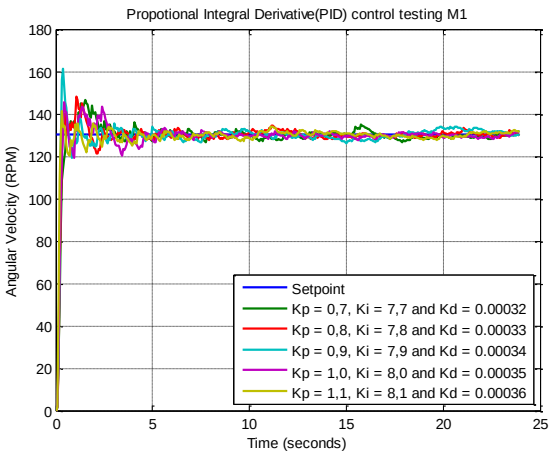

Fig. 17. . 1 Motor M1 Response Kpid Graph

TABLE IX. TESTING PROPOTIONAL INTEGRAL DERIVATIVE (PID) CONTROL M2

Propotiona Integral Derivative (PID) control testing M2								
No .	Kp	Ki	Kd	Rise Time (Tr)	Overshoot (Mp)	Peak Time (Ts)	Settling Time (Ts)	Steady State error
1	0.6	9.1	0.00006	0.56	12.33	2.1	7.36	-0.88
2	0.7	9.2	0.00007	0.49	11.16	1.38	7.54	1.85
3	0.8	9.3	0.00008	0.34	15.41	0.54	20.22	-0.03
4	0.9	9.4	0.00009	0.38	5.5	2.88	13.24	-0.16
5	1	9.5	0.0001	0.25	7.67	0.6	21.72	0.73

It can be seen in table 4.10 the response to get parameters for motor 2 Kpid with the value of Kp = 0.9; Ki = 9.4; Kd = 0.0009 with a rise time of 0.38/second; overshoot 5.5; peak time 2.88/second; settling time 13.24/second, and steady state error -0.16 with time to stabilize faster than other parameters. And can be seen the response of motor 2 with the form of a graph that can be seen in Figure 19.

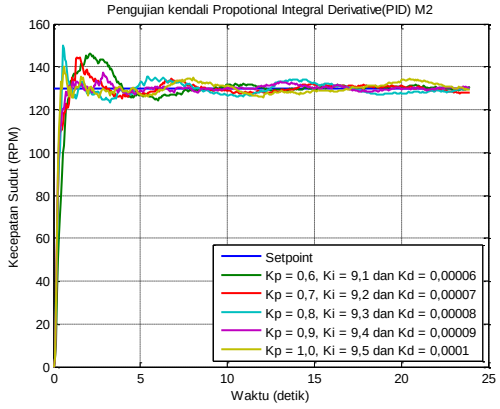

Fig. 18. Motor M2 Response Kpid Graph

4. Disturbance testing of PID response

Disturbance testing of the response of motors M1 and M2 to PWM 50 with a hall magnetic rotary encoder sensor which is in the form of steering represented by the value in the program, namely angle_R (right turn Y = 0˚ > -45˚) to affect motor M1 and angle_L (left turn Y = -45˚ < 0) to affect motor M2, while producing a drivetrain which if simulated when the angle_R is Y = 0˚ > -45˚, the speed of the M1 motor will decrease along with the PWM value also decreases along with the voltage decreases, otherwise the M2 motor will experience an increase in speed and voltage increases. Likewise, when the angle_L value is Y = -45˚ < 0˚, it will be inversely proportional, the M2 motor speed will decrease along with the PWM value also decreases while the voltage decreases, otherwise the M1 motor will experience an increase in PWM, speed, voltage increases. The test results of angle_R interference in Table 10 and the test results of angle_L interference in Table 11 are in the form of voltage.

TABLE X. ARC TESTING OF ANGLE_R AGAINST MOTOR VOLTAGE M1&M2

Testing Arc angle_R degree against Motor voltage				
No.	Right°	Motor 1 V	Left°	Motor 2 V
1	-5	2.5	-5	2.6
2	-10	2.3	-10	2.8
3	-15	2.1	-15	3
4	-20	1.9	-20	3.2
5	-45	1.7	-45	3.4

TABLE XI. ARC TESTING OF ANGLE_L AGAINST MOTOR VOLTAGE M1&M2

Testing Arc angle_L degree against Motor voltage				
No.	Right°	Motor 1 V	Left°	Motor 2 V
1	-5	2.6	-5	2.5
2	-10	2.8	-10	2.3
3	-15	3	-15	2.1
4	-20	3.2	-20	1.9
5	-45	3.4	-45	1.7

From the interference test, the motor response can also be seen in Table 12 and Figure 20.

TABLE XII. M1&M PROPOTIONAL INTEGRAL DERIVATIVE (PID) CONTROL DISTURBANCE TESTING

Pengujian kendali Propotiona Integral Derivative Terbaik (PID) M1&M2								
Mtr	Kp	Ki	Kd	Rise Time (Tr)	Overshoot (Mp)	Peak Time (Ts)	Settling Time (Ts)	Steady State error
M1	1.1	8.1	0.00036	0.27044704	19.3230769	2.64	23.76125	-0.08
M2	0.9	9.4	0.00009	0.16911405	15.1153846	1.56	23.836	1.11

Seen from Table 12 M1 motor with parameters Kp = 1.1; Ki = 8.1; Kd = 0.00036 with angle_R disturbance (right turn Y = 0˚ > -45˚) produces rise time 0.27/second; overshoot 19.32; peak time 2.64; settling time 23.76; steady state error -0.08% and M2 motor with parameters Kp = 0.9; Ki = 9.4; Kd = 0.00009 with an angle disturbance_L (left turn Y = -45˚ > 0˚) produces a rise time of 0.16/second; overshoot 15.11; peak time 1.56; settling time 23.83; steady state error -1.11%, it can be concluded that the parameters obtained by the motor response are quite good in overcoming the given disturbance even though the settling time value is not fast enough to stabilize the motor response.

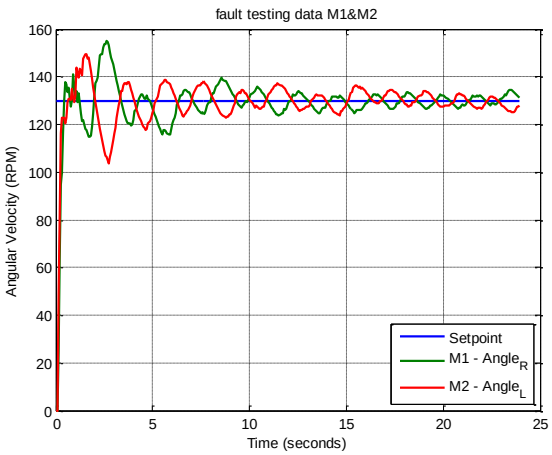

Fig. 19. Disturbance Graph of PID M1&M2

IV. CONCLUSION

Research was conducted to control two motors so that the speed of motor 1 and motor 2 has the same speed with a setpoint of 130 RPM. In this case, the use of the kalman filter method is used to eliminate the noise/noise of the rotary encoder sensor output to read the sensor speed angle in RPM units with a multiplier value of countPulseM1 = 20.0 and countPulseM2 = 40.9. The difference in multiplier values is due to different pulse readings between motor 1 and motor 2 getting the ratio value of the kalman filter parameter variation of motor 1 (R = 10.0; Q = 0.0001) and motor 2 (R = 8.0; Q = 0.0001) from such a large ratio causing slow motor response.

The third test using a ratio of R = 10; Q = 0.0001 on M1 and a ratio of R = 8.0; Q = 0.0001 on M2 is the best ratio value that can reduce noise that is too high but the response is so slow. Compared to the first and second tests with the ratio of R = 8.0; Q = 0.01 and R = 9.5; Q = 0.001 on M1 and the ratio for M2 R = 7.0; Q = 0.01 and R = 7.5; Q = 0.001.

From the response of the two motors that are so slow from the results of the large ratio value of kalman filter parameters, it is improved using the PID method with the results of try and error parameter variations to get the best PID parameter values for motor 1 Kp = 1.1; Ki = 8.1; Kd = 0.00036 and motor 2 parameters Kp = 1.1; Ki = 8.1; Kd = 0.00036 with a rise time of 0.13/second; overshoot 8.69; peak time 141.62; 11.4% and steady state error -1.19.

The PID parameters of the two DC motors obtained were tested again by giving a disturbance using a hall magnetic rotary encoder sensor as a steering wheel, Motor M1 with parameters Kp = 1.1; Ki = 8.1; Kd = 0.00036. Experiencing angle_R disturbance (turning to the right Y = 0˚ to -45˚) results in a rise time of 0.27 seconds; overshoot 19.32; peak time 2.64; settling time 23.76, and steady state error -0.08%. Meanwhile, the M2 motor with parameters Kp = 0.9; Ki = 9.4; Kd = 0.00009. Experiencing an angle_L disturbance (turning left Y = -45˚ to 0˚) results in a rise time of 0.16 seconds; overshoot 15.11; peak time 1.56; settling time 23.83 and steady state error -1.11%. It can be concluded that the parameters used provide a fairly good motor response in overcoming the given disturbance, although the settling time value is still not fast enough to stabilize the motor response.

REFERENCES

[1] Q. Ariyansyah and A. Ma'arif, "DC Motor Speed Control with Proportional Integral Derivative (PID) Control on the Prototype of a Mini-Submarine," *JFSC*, vol. 1, no. 1, pp. 18–24, 2023, https://doi.org/10.59247/jfsc.v1i1.26.

[2] A. J. Attiya, Y. Wenyu, S. W. Shneen "PSO_PI controller of robotic grinding force servo system," *TELKOMNIKA Indonesian Journal of Electrical Engineering*, vol. 15, no. 3, pp. 515-525, 2015, http://doi.org/10.11591/tijee.v15i3.1570.

[3] M. Alfiyan and R. D. Puriyanto, "Mecanum 4 Omni Wheel Directional Robot Design System Using PID Method," *JFSC*, vol. 1, no. 1, pp. 6–13, 2023, https://doi.org/10.59247/jfsc.v1i1.27.

[4] A. J. Attiya, S. W. Shneen, B. A. Abbas, Y. Wenyu, "Variable speed control using fuzzy-pid controller for two-phase hybrid stepping motor in robotic grinding," *Indonesian Journal of Electrical Engineering and Computer Science*, vol. 3, no. 1, pp. 102-118, 2016, https://doi.org/10.11591/ijeecs.v3.i1.pp102-118.

[5] A. J. Attiya, Y. Wenyu, S. W. Shneen, "Compared with PI, Fuzzy-PI and PSO-PI controllers of robotic grinding force servo system," *TELKOMNIKA Indonesian Journal of Electrical Engineering*, vol. 16, no. 1, pp. 65-74, 2015, https://doi.org/10.11591/tijee.v16i1.1589.

[6] A. J. Attiya, Y. Wenyu, S. W. Shneen, "Fuzzy-PID controller of robotic grinding force servo system," *TELKOMNIKA Indonesian Journal of Electrical Engineering*, vol. 15, no. 1, pp. 87-99, 2015, https://doi.org/10.11591/telkomnika.v15i1.8051.

[7] H. Maghfiroh, J. Slamet Saputro, F. Fahmizal, and M. Ahmad Baballe, "Adaptive Fuzzy-PI for Induction Motor Speed Control," *JFSC*, vol. 1, no. 1, pp. 1–5, 2023, https://doi.org/10.59247/jfsc.v1i1.24.

[8] Fahmizal, D. Yanu Kharisma, and S. Pramono, "Implementation of Fuzzy Logic Control on a Tower Copter," *JFSC*, vol. 1, no. 1, pp. 14–17, 2023, https://doi.org/10.59247/jfsc.v1i1.25.

[9] M. A. Al-bahrany and A. T. A. Sadda, "Smart Dc to DC converter for a Small Drone Based upon Deep Learning Technique," *JFSC*, vol. 1, no. 2, pp. 55–60, 2023, https://doi.org/10.59247/jfsc.v1i2.43.

[10] H. Maghfiroh, C. Hermanu, M. H. Ibrahim, M. Anwar, A. Ramelan, "Hybrid fuzzy-PID like optimal control to reduce energy consumption," *TELKOMNIKA (Telecommunication Computing Electronics and Control)*, vol. 18, no. 4, pp. 2053-2061, 2020, http://doi.org/10.12928/telkomnika.v18i4.14535.

[11] H. S. Dakheel, Z. B. Abdullah, N. S. Jasim, S. W. Shneen, "Simulation model of ANN and PID controller for direct current servo motor by using Matlab/Simulink," *TELKOMNIKA (Telecommunication Computing Electronics and Control)*, vol. 20, no. 4, pp. 922-932, 2022, http://doi.org/10.12928/telkomnika.v20i4.23248.

[12] S. W. Shneen, H. S. Dakheel, Z. B. Abdullah, "Design and Implementation of No Load, Constant and Variable Load for DC Servo Motor." *Journal of Robotics and Control (JRC)*, vol. 4, no. 3, pp. 323-329, 2023, https://doi.org/10.18196/jrc.v4i3.17387.

[13] H. Maghfiroh, I. Iftadi, A. Sujono, "Speed control of induction motor using LQG," *Journal of Robotics and Control (JRC)*, vol. 2, no. 6, pp. 565-570, 2021, https://doi.org/10.18196/26138.

[14] H. Maghfiroh, M. Nizam, M. Anwar and A. Ma'Arif, "Improved LQR Control Using PSO Optimization and Kalman Filter Estimator," *IEEE Access*, vol. 10, pp. 18330-18337, 2022, https://doi.org/10.1109/ACCESS.2022.3149951.

[15] H. Maghfiroh, A. Ma'arif, F. Adriyanto, I. Suwarno, W. Caesarendra, "Adaptive Linear Quadratic Gaussian Speed Control of Induction Motor Using Fuzzy Logic," *Journal Européen des Systèmes Automatisés*, vol. 56, no. 4, pp. 703-711, 2023, https://doi.org/10.18280/jesa.560420.

[16] H. S. Dakheel, Z. B. Abdullah, N. S. Jasim, S. W. Shneen, "Simulation model of ANN and PID controller for direct current servo motor by using Matlab/Simulink," *TELKOMNIKA (Telecommunication Computing Electronics and Control)*, vol. 20, no. 4, pp. 922-932, 2022, http://doi.org/10.12928/telkomnika.v20i4.23248.

[17] S. Waley, C. Mao, N. K. Bachache, "Biogeography based optimization tuned fuzzy logic controller to adjust speed of electric vehicle," *TELKOMNIKA Indonesian Journal of Electrical Engineering*, vol. 16, no. 3, pp. 509-519, 2015, http://doi.org/10.11591/tijee.v16i3.1642.

[18] A. Batool, N. U. Ain, A. A. Amin, M. Adnan, M. H. Shahbaz, "A comparative study of DC servo motor parameter estimation using

various techniques," *Automatika*, vol. 63, no. 2, pp. 303-312, 2022, https://doi.org/10.1080/00051144.2022.2036935.

[19] D. Saputra, A. Ma'arif, H. Maghfiroh, P. Chotikunnan, S. N. Rahmadhia, "Design and Application of PLC-based Speed Control for DC Motor Using PID with Identification System and MATLAB Tuner," *International Journal of Robotics and Control Systems*, vol. 3, no. 2, pp. 233-244, 2023, https://doi.org/10.31763/ijrcs.v3i2.775.

[20] A. Ma'arif, I. Suwarno, H. Maghfiroh, W. Rahmaniar, A. A. Nuryono and N. M. Raharja, "Sliding Mode Control of Angular Speed DC Motor System with Parameter Uncertainty," *2022 IEEE International Conference on Communication, Networks and Satellite (COMNETSAT)*, pp. 380-387, 2022, https://doi.org/10.1109/COMNETSAT56033.2022.9994286.

[21] A. Ma'arif, N. R. Setiawan, "Control of DC motor using integral state feedback and comparison with PID: simulation and arduino implementation," *Journal of Robotics and Control (JRC)*, vol. 2, no. 5, pp. 456-461, 2021, https://doi.org/10.18196/jrc.25122.

[22] P. Ramesh Babu and V. Prabhu, "Modeling and performance analysis of Buck Converter fed PMBLDC Motor Drives in Matlab/Simulink environment," *2013 International Conference on Circuits, Power and Computing Technologies (ICCPCT)*, pp. 219-224, 2013, https://doi.org/10.1109/ICCPCT.2013.6529014.

[23] R. Kristiyono, Wiyono, "Autotuning Fuzzy PID Controller for Speed Control of BLDC Motor," *Journal of Robotics and Control (JRC)*, vol. 2, no. 5, pp. 400-407, 2021, https://doi.org/10.18196/jrc.25114.

[24] S. W. Shneen, H. S. Dakheel, Z. B. Abdulla, "Advanced Optimal for PV system coupled with PMSM," *Indonesian Journal of Electrical Engineering and Computer Science*, vol. 1, no. 3, pp. 556-565, 2016, https://doi.org/10.11591/ijeecs.v1.i3.pp556-565.

[25] A. Muttaqin, S. D. Finnadi, Z. Abidin, K. Araki, "FPGA based synchronous multi-channel PWM generator for humanoid robot," *International Journal of Electrical & Computer Engineering*, vol. 11, no. 1, pp. 2088-8708, 2021, http://doi.org/10.11591/ijece.v11i1.pp249-256.

[26] A. S. Ahmed, H. A. Marzog, L. A. A. Rahaim, "Design and implement of robotic arm and control of moving via IoT with Arduino ESP32," *International Journal of Electrical & Computer Engineering*, vol. 11, no. 5, pp. 2088-8708, 2021, http://doi.org/10.11591/ijece.v11i5.pp3924-3933.

[27] S. W. Shneen, G. A. Aziz, "Simulation model of 3-phase PWM rectifier by using MATLAB/Simulink," *International Journal of Electrical and Computer Engineering*, vol. 11, no. 5, p. 3736, 2021, http://doi.org/10.11591/ijece.v11i5.pp3736-3746.

[28] D. H. Shaker, S. W. Shneen, F. N. Abdullah, G. A. Aziz, "Simulation Model of Single-Phase AC-AC Converter by Using MATLAB," *Journal of Robotics and Control (JRC)*, vol. 3, no. 5, pp. 656-665, 2022, https://doi.org/10.18196/jrc.v3i5.15213.

[29] N. Salem, K. Mateen, W. Alharbi and J. Kamal, "Performance of LQR and PID Controllers for RS-550VC Motor Speed Enhancement," *2023 6th International Conference on Intelligent Robotics and Control Engineering (IRCE)*, pp. 01-06, 2023, https://doi.org/10.1109/IRCE59430.2023.10255039.

[30] A. L. Shuraiji, S. W. Shneen, "Fuzzy Logic Control and PID Controller for Brushless Permanent Magnetic Direct Current Motor: A Comparative Study," *Journal of Robotics and Control (JRC)*, vol. 3, no. 6, pp. 762-768, 2022, https://doi.org/10.18196/jrc.v3i6.15974.

[31] J. A. Mohammed, A. L. Shuraiji, "Modeling of DC elevator motor drive for mid-rise building," *Engineering & Technology Journal*, vol. 31, no. 12, pp. 2320-2342, 2013, https://doi.org/10.30684/etj.31.12A.10.

[32] G. A. Aziz, S. W. Shneen, F. N. Abdullah, D. H. Shaker, "Advanced optimal GWO-PID controller for DC motor," *Int. J. Adv. Appl. Sci.*, vol. 11, no. 3, pp. 263-276, 2022, http://doi.org/10.11591/ijaas.v11.i3.pp263-276.

[33] Y. Zhu, X. He, Q. Liu, W. Guo, "Semiclosed-loop motion control with robust weld bead tracking for a spiral seam weld beads grinding robot," *Robotics and Computer-Integrated Manufacturing*, vol. 73, p. 102254, 2022, https://doi.org/10.1016/j.rcim.2021.102254.

[34] H. Maghfiroh, M. Ahmad, A. Ramelan, F. Adriyanto, "Fuzzy-PID in BLDC Motor Speed Control Using MATLAB/Simulink," *Journal of Robotics and Control (JRC)*, vol. 3, no. 1, pp. 8-13, 2022, https://doi.org/10.18196/jrc.v3i1.10964.

[35] S. W. Jeaeb, A. Z. Salman, Q. A. Jawad, H. Shareef, "Advanced optimal by PSO-PI for DC motor," *Indonesian Journal of Electrical Engineering and Computer Science*, vol. 16, no. 1, pp. 165-175, 2019, http://doi.org/10.11591/ijeecs.v16.i1.pp165-175.

[36] A. Latif, A. Z. Arfianto, H. A. Widodo, R. Rahim, E. T. Helmy, "Motor DC PID system regulator for mini conveyor drive based-on MATLAB," *Journal of Robotics and Control (JRC)*, vol. 1, no. 6, pp. 185-190, 2020, https://doi.org/10.18196/jrc.1636.

[37] H. J. Pahk, D. S. Lee, J. H. Park, "Ultra precision positioning system for servo motor–piezo actuator using the dual servo loop and digital filter implementation," *International Journal of Machine Tools and Manufacture*, vol. 41, no. 1, pp. 51-63, 2001, https://doi.org/10.1016/S0890-6955(00)00061-4.

[38] M. L. Zegai, M. Bendjebbar, K. Belhadri, M. L. Doumbia, B. Hamane and P. M. Koumba, "Direct torque control of Induction Motor based on artificial neural networks speed control using MRAS and neural PID controller," *2015 IEEE Electrical Power and Energy Conference (EPEC)*, pp. 320-325, 2015, https://doi.org/10.1109/EPEC.2015.7379970.

[39] Z. B. Abdullah, S. W. Shneen, H. S. Dakheel, "Simulation Model of PID Controller for DC Servo Motor at Variable and Constant Speed by Using MATLAB," *Journal of Robotics and Control (JRC)*, vol. 4, no. 1, pp. 54-59, 2023, https://doi.org/10.18196/jrc.v4i1.15866.

[40] G. Boukhalfa, S. Belkacem, A. Chikhi, S. Benaggoune, "Direct torque control of dual star induction motor using a fuzzy-PSO hybrid approach," *Applied Computing and Informatics*, vol. 18, no. 1/2, pp. 74-89, 2020, https://doi.org/10.1016/j.aci.2018.09.001.

[41] A. R. Ajel, H. M. A. Abbas, M. J. Mnati, "Position and speed optimization of servo motor control through FPGA," *International Journal of Electrical & Computer Engineering*, vol. 11, no. 1, pp. 2088-8708, 2021, http://doi.org/10.11591/ijece.v11i1.pp319-327.

[42] A. N. Abdullah, M. H. Ali, "Direct torque control of IM using PID controller," *International Journal of Electrical and Computer Engineering*, vol. 10, no. 1, p. 617, 2020, http://doi.org/10.11591/ijece.v10i1.pp617-625.

[43] H. S. Dakheel, Z. B. Abdullah, S. W. Shneen, "Advanced optimal GA-PID controller for BLDC motor," *Bulletin of Electrical Engineering and Informatics*, vol. 12, no. 4, pp. 2077-2086, 2023, https://doi.org/10.11591/eei.v12i4.4649.

[44] B. B. Acharya, S. Dhakal, A. Bhattarai, N. Bhattarai, "PID speed control of DC motor using meta-heuristic algorithms," *International Journal of Power Electronics and Drive Systems*, vol. 12, no. 2, p. 822, 2021, http://doi.org/10.11591/ijpeds.v12.i2.pp822-831.

[45] F. N. Abdullah, G. A. Aziz, S. W. Shneen, "Simulation Model of Servo Motor by Using Matlab," *Journal of Robotics and Control (JRC)*, vol. 3, no. 2, pp. 176-179, 2022, https://doi.org/10.18196/jrc.v3i2.13959.

[46] S. Usha, P. M. Dubey, R. Ramya, M. V. Suganyadevi, "Performance enhancement of BLDC motor using PID controller," *International Journal of Power Electronics and Drive Systems*, vol. 12, no. 3, 2021, https://doi.org/10.11591/ijpeds.v12.i3.pp1335-1344.

[47] G. Boukhalfa, S. Belkacem, A. Chikhi, S. Benaggoune, "Genetic algorithm and particle swarm optimization tuned fuzzy PID controller on direct torque control of dual star induction motor," *Journal of Central South University*, vol. 26, no. 7, pp. 1886-1896, 2019, https://doi.org/10.1007/s11771-019-4142-3.

[48] S. W. Shneen, D. H. Shaker, F. N. Abdullah, "Simulation model of PID for DC-DC converter by using MATLAB," *International Journal of Electrical and Computer Engineering*, vol. 11, no. 5, p. 3791, 2021, https://doi.org/10.11591/ijece.v11i5.pp3791-3797.

[49] S. W. Shneen, F. N. Abdullah, D. H. Shaker, "Simulativ on model of single phase PWM inverter by using MATLAB/Simulink," *International Journal of Power Electronics and Drive Systems*, vol. 12, no. 1, p. 212, 2021, http://doi.org/10.11591/ijpeds.v12.i1.pp212-216.

[50] S. W. Shneen, H. S. Dakheel, Z. B. Abdulla, "Design and implementation of variable and constant load for induction motor," *International Journal of Power Electronics and Drive Systems*, vol. 11, no. 2, p. 762, 2020, http://doi.org/10.11591/ijpeds.v11.i2.pp762-773.